

## Biosorption potential of *Sapindus mukorossi* dead leaves as a novel biosorbent for the treatment of Reactive Red 241 in aqueous solution

Farhan Javed<sup>a,\*</sup>, Nadeem Feroze<sup>b</sup>, Amir Ikhtlaq<sup>c,\*</sup>, Mohsin Kazmi<sup>d</sup>, Syed Waqas Ahmad<sup>a</sup>, Hafiz Muhammad Shahzad Munir<sup>b</sup>

<sup>a</sup>Department of Chemical and Polymer Engineering, University of Engineering and Technology, Lahore, FSD Campus 38000, Pakistan, Tel. +92412433508; email: farhan.javed@uet.edu.pk (F. Javed), Tel. +92412433500; email: syed.waqas.ahmad@gmail.com (S.W. Ahmad)

<sup>b</sup>Department of Chemical Engineering, University of Engineering and Technology, Lahore 54890, Pakistan, Tel. +924299029230; email: drnchohan@yahoo.com (N. Feroze), engrsm124@gmail.com (H.M.S. Munir)

<sup>c</sup>Institute of Environmental Engineering and Research, University of Engineering and Technology, Lahore 54890, Pakistan, Tel. +924299029248; email: aamirikhlaq@uet.edu.pk

<sup>d</sup>Department of Chemical Engineering, University of Engineering and Technology, Lahore, KSK Campus 39020, Pakistan, Tel. +924235515684; email: engr.smalikazmi@gmail.com

Received 14 March 2018; Accepted 20 September 2018

---

### ABSTRACT

The research work focuses on the assessment of biosorption potential of *Sapindus mukorossi* dead leaves (SMDL) as a novel, cheaper, and abundantly available biosorbent for the treatment of C.I. Reactive red 241 (RR-241) in aqueous solution. The biosorbent characterization was performed by using scanning electron microscopy, Fourier transform infrared spectroscopy, energy dispersive X-ray, and Brunauer–Emmett–Teller surface area analysis techniques. The dye biosorption was studied as a function of various operating parameters including initial pH, adsorbent dose, dye concentration, adsorption time, and temperature. Moreover, kinetic modeling was conducted by implying pseudo-first-order kinetic model, pseudo-second-order kinetic model, Elovich, and intraparticle diffusion models. The Langmuir, Freundlich, Temkin, and Dubinin–Radushkevich models were applied for adsorption isotherm modeling. Finally, the thermodynamic parameters like the difference in free energy ( $\Delta G^\circ$ ) was evaluated by Gibb's equation while the difference in enthalpy ( $\Delta H^\circ$ ) and entropy ( $\Delta S^\circ$ ) was evaluated by Van't Hoff equation. The results show that more than 95% dye removal efficiency was achieved on SMDL with an equilibrium capacity of 8.18 mg/g. The results further exposed that the biosorption of RR-241 on SMDL pursued pseudo-second-order kinetics ( $R^2 = 0.99$ ). The adsorption isotherms gave the best fit with the Freundlich model ( $R^2 = 0.99$ ). The negative free energy change ( $\Delta H^\circ$ ) values confirmed spontaneous and feasible adsorption. The positive values of enthalpy change ( $\Delta H^\circ = 14.39$  kJ/mol) indicated the endothermic adsorption nature and entropy change ( $\Delta S^\circ = 0.055$  kJ/mol/K) indicated the increased randomness at the solid–liquid interface. It is concluded that the SMDL has a good biosorption potential as low-cost biosorbent for the abatement of RR-241 in aqueous solutions.

**Keywords:** Biosorption; *Sapindus mukorossi* dead leaves; Reactive red

---

\* Corresponding author.

## 1. Introduction

The water resources are being continuously contaminated by industrial wastewater which has become a matter of concern due to hazardous environmental impacts [1]. The industrial wastewater, a composing mixture of various pollutants of organic and inorganic nature requires proper treatment prior to discharging into the environment [2,3]. Synthetic dyes are among the major organic pollutants found in industrial wastewaters such as textile, food, paper, rubber, cosmetic, and leather [3]. About 60%–70% of synthetic dyes are azo dyes having certain qualities of chemical stability, brightness, and color fastness [4]. The complex conjugated ring structure and synthetic origin make dyes recalcitrant [5]. Therefore, the treatment of colored wastewater is necessary due to adverse mutagenic, carcinogenic, and toxic effects on the aquatic life and human beings [6].

Numerous treatment methods have been studied for the removal of color such as adsorption [2], electrochemical techniques [7], advanced oxidation processes [8], coagulation–flocculation [9], biological treatment [10], and membrane separation [11]. Among these, adsorption has become a versatile technique owing to its flexibility, low cost, high removal efficiency, nontoxicity, and regeneration [12–15]. A continuous quest for low cost and environment-friendly adsorbents has led researchers to use biosorbents. Various plant based lignocellulosic materials have been studied as economical, renewable, and biodegradable sorbents for the treatment of colored wastewater such as bagasse [16], plant leaves [17], peanut shell [2], saw dust [18], and fruit shell [19]. The plant-based materials are effective biosorbents for pollutants abatement due to diverse active functional groups present at their surfaces such as hydroxyl, amino, and carboxyl groups [2]. Thus, act as low cost, abundantly available, and environment-friendly biosorbents for dye removal.

In current investigation C.I. Reactive red 241 (RR-241) was selected as a model textile dye. The RR-241 is an anionic reactive mono-chloro triazine azo synthetic water soluble dye, containing sulfonic acid auxochrome and azo group chromogen, vastly applied for the coloration of cotton, silk, and wool [20]. Reactive dyes have lower fixation rates and about 10%–50% dye is lost in effluents. The recalcitrant nature of reactive dyes poses a threat to the environment as its exposure leads to cancer, skin allergies, dermatitis, kidney and nervous system damage, respiration problems in human beings, and may destroy aquatic life [9]. The average dye concentration in the industrial dye house varies from 0.01 to 0.25 g/L [20] and the color discharge limit is 80 Pt-Co [20].

Current attempt targets to evaluate the efficiency of novel dead leaves of *Sapindus mukorossi* as a cheap novel biosorbent for the treatment of a model anionic dye (RR-241). To the best of author's knowledge, *Sapindus mukorossi* dead leaves (SMDL) have not been previously studied for the treatment of dyes. The abundance availability of SMDL brings about an economical option for the treatment of dyes by adsorption. The work involves the application of an agricultural waste material (SMDL) as a novel, natural biosorbent for the treatment of a hazardous dye as a step toward effective utilization of waste materials. In the current investigation, the influence of operational factors such as initial pH, SMDL dosage, initial RR-241 concentration, treatment time,

and temperature on the biosorption was elucidated. The adsorption kinetics was elucidated by applying the pseudo-first-order kinetic model, pseudo-second-order kinetic model, Elovich, and intraparticle diffusion models. Isotherm studies were performed by applying Langmuir, Freundlich, Temkin, and Dubinin–Radushkevich (D-R) isotherm models and thermodynamics was also investigated. Adsorption thermodynamic parameters such as free energy difference ( $\Delta G^\circ$ ), enthalpy difference ( $\Delta H^\circ$ ), and entropy difference ( $\Delta S^\circ$ ) were also evaluated.

## 2. Material and methods

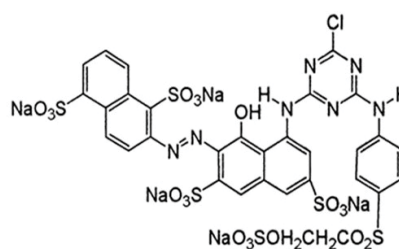
### 2.1. Chemicals

The C.I. Reactive Red 241 dye was provided by Archroma (Switzerland) and was used in this work without further purification. The analytical grade Sodium chloride, HCl, and NaOH were purchased from Merck (Germany). All the chemicals utilized in this research work were of analytical grade. The chemical properties and structure of the dye are shown in Fig. 1.

### 2.2. Adsorbent preparation and characterization

The dead leaves of *S. mukorossi* were collected from the vicinity of local trees of *S. mukorossi*. The leaves were first washed with ultrapure deionized water to eliminate the dirt and extraneous material, then washed multiple times with ultrapure deionized water until neutral pH of wash water was obtained. The washed leaves were air dried first at room temperature and subsequently oven dried at 60°C for 24 h to remove all moisture. The dried leaves were grinded using a grinder and then sieved through 80 mesh sieve to obtain a particle size of <177  $\mu\text{m}$  and the obtained SMDL adsorbent powder was stored in an air tight container.

The adsorbent surface functional groups were elucidated by Fourier transform infrared spectrometer (FTIR, Bruker, Alpha-E) in the range 500–4,000  $\text{cm}^{-1}$ . The surface morphology and microstructure of biosorbent was characterized by scanning electron microscope (SEM) loaded with an energy dispersive X-ray (EDX) spectrometer (Tescan, Vega LMU). The physical properties of the adsorbent such as the specific surface area of the biosorbent, total pore volume, and pore size were evaluated by Brunauer–Emmett–Teller (BET) surface area and pore size analyzer (Quantachrome, NOVA1200e).



Commercial Name: Drimaren Red CL-5B Type: Anionic monoazo reactive dye  
 Chemical Formula:  $\text{C}_{31}\text{H}_{19}\text{ClN}_7\text{Na}_5\text{O}_{19}\text{S}_6$  Molecular weight: 1136 g/mol  
 $\lambda_{\text{max}}$ : 542nm

Fig. 1. Properties and structure of RR-241.

The biosorbent point of zero charge was assessed by the pH drift method [21].

### 2.3. Adsorption experiments

Experiments were executed in various 250 mL Erlenmeyer flasks holding 50 mL batches of dye solution of desired concentration. A stock solution of dye (100 mg/L) was formulated by adding the weighed amount of dye in deionized water. The desired dye solutions of required concentration were prepared by the dilution of stock solution with deionized water. The desired quantity of adsorbent was put in the dye solution and agitation was provided at 200 rpm using water bath orbital shaker (Model Benchmark Scientific SB08) at a fixed temperature ( $30^{\circ}\text{C} \pm 0.5^{\circ}\text{C}$ ). The initial pH of the dye solution was set to desired values by adding 0.1 M NaOH or 0.1 M HCl solutions, using pH meter (Model Hanna HI9811-5). The adsorption parameters of pH, SMDL dose, and initial concentration of dye solution with time and temperature were studied. The dye samples were withdrawn after regular time intervals, filtered through 0.45  $\mu\text{m}$  pore size membrane filter and the concentration of the dye was then analyzed by double beam UV-Vis spectrophotometer (Perkin Elmer Lambda 35). The dye percentage removal was determined by the following equation:

$$\text{Dye removal (\%)} = \frac{C_o - C_t}{C_o} \times 100 \quad (1)$$

where  $C_o$  and  $C_t$  are the RR-241 concentration at the start (mg/L) and at time  $t$ , respectively. The adsorption capacity was determined by the following equations:

$$q_t = \frac{(C_o - C_t)V}{M} \quad (2)$$

$$q_e = \frac{(C_o - C_e)V}{M} \quad (3)$$

where  $q_t$  and  $q_e$  are the adsorption capacities (mg/g) at time  $t$  and equilibrium, respectively.  $C_o$ ,  $C_t$ , and  $C_e$  are the RR-241 concentrations at the start, at time  $t$ , and equilibrium (mg/L), respectively.  $M$  is the mass of biosorbent (g) and  $V$  is the volume of the aqueous dye solution (L).

### 2.4. Adsorption kinetics

The kinetic experiments were conducted as described earlier, by taking 50 mL RR-241 solution in Erlenmeyer flasks with initial dye concentrations of 10, 30, 50, and 70 mg/L, then a constant quantity of biosorbent was added and a decrease in dye concentration with time was noted. The adsorption mechanism was studied by applying four kinetics models on biosorption of RR-241 on SMDL, these were pseudo-first-order kinetic model, pseudo-second-order kinetic model, Elovich model, and intraparticle diffusion model.

The equation for pseudo-first-order kinetic model as described by Ref. [22] is represented as follows:

$$\frac{dq_t}{dt} = K_1(q_e - q_t) \quad (\text{Nonlinear form}) \quad (4)$$

$$\ln(q_e - q_t) = \ln q_e - K_1 t \quad (\text{Linear form}) \quad (5)$$

The pseudo-first-order kinetic model attributes the adsorbent-adsorbate interaction to the physical forces of attraction.

The equation representing the pseudo-second-order kinetic model as described by Ref. [23] is as follows:

$$\frac{dq_t}{dt} = K_2(q_e - q_t)^2 \quad (\text{Nonlinear form}) \quad (6)$$

$$\frac{t}{q_t} = \frac{1}{K_2 q_e^2} + \frac{t}{q_e} \quad (\text{Linear form}) \quad (7)$$

The initial biosorption rate of second-order kinetic model is represented by  $h$  (mg/g min) given by the following equation:

$$h = K_2 q_e^2 \quad (8)$$

The Elovich model equation for kinetic studies as described by Ref. [24] is represented as follows:

$$\frac{dq_t}{dt} = \alpha e^{-\beta q_t} \quad (\text{Nonlinear form}) \quad (9)$$

$$q_t = \frac{1}{\beta} \ln(\alpha\beta) + \frac{1}{\beta} \ln(t) \quad (\text{Linear form}) \quad (10)$$

The intraparticle diffusion model kinetic equation as described by Ref. [25] is represented as follow:

$$q_t = K_{\text{dif}} t^{1/2} + C \quad (\text{Linear form}) \quad (11)$$

### 2.5. Adsorption isotherms

The equilibrium data were fitted to adsorption isotherms on the biosorption of reactive red 241 on SMDL to elucidate the equilibrium relationship between the sorbent and sorbate.

The Langmuir isotherm model assuming the monolayer homogeneous adsorption is represented by the following equation [26]:

$$q_e = \frac{K_L q_m C_e}{1 + K_L C_e} \quad (\text{Nonlinear form}) \quad (12)$$

$$\frac{C_e}{q_e} = \frac{1}{K_L q_m} + \frac{C_e}{q_m} \quad (\text{Linear form}) \quad (13)$$

The dimensionless separation factor is given by the following equation:

$$R_L = \frac{1}{1 + K_L C_o} \quad (14)$$

The Freundlich isotherm model assuming the heterogeneous adsorption is represented by the following equation [27]:

$$q_e = K_F C_e^{1/n} \quad (\text{Nonlinear form}) \quad (15)$$

$$\ln q_e = \ln K_F + \frac{1}{n} \ln C_e \quad (\text{Linear form}) \quad (16)$$

The Temkin isotherm model that gives the relationship between the amount of dye adsorbed and heat of adsorption is represented by the following equation [28]:

$$q_e = \frac{RT}{b} \ln(K_T C_e) \quad (\text{Nonlinear form}) \quad (17)$$

$$q_e = \frac{RT}{b} \ln K_T + \frac{RT}{b} \ln C_e \quad (\text{Linear form}) \quad (18)$$

The D-R isotherm model is represented mathematically as follows [29]:

$$q_e = q_m e^{-\beta \epsilon^2} \quad (\text{Nonlinear form}) \quad (19)$$

$$\ln q_e = \ln q_m - \beta \epsilon^2 \quad (\text{Linear form}) \quad (20)$$

$$\epsilon = RT \ln \left( 1 + \frac{1}{C_e} \right) \quad (21)$$

### 2.6. Adsorption thermodynamics

Adsorption thermodynamics elucidate the adsorption mechanism by adsorption parameters such as free energy difference ( $\Delta G^\circ$ ), enthalpy difference ( $\Delta H^\circ$ ), and entropy difference ( $\Delta S^\circ$ ), which give an insight into the energy changes involved in the adsorption process. The free energy change ( $\Delta G^\circ$ ) is the indicator for the adsorption spontaneity and feasibility and is determined by the Gibbs equation represented by the following equation [18]:

$$\Delta G = -RT \ln \left( \frac{q_e}{C_e} \right) \quad (22)$$

The enthalpy difference ( $\Delta H^\circ$ ) indicates the nature of adsorption being exothermic or endothermic, while the entropy difference ( $\Delta S^\circ$ ) indicates changes in the degree of randomness. The enthalpy change ( $\Delta H^\circ$ ) and entropy difference ( $\Delta S^\circ$ ) can be assessed from the plot of Van't Hoff equation represented as follows [18]:

$$\ln \left( \frac{q_e}{C_e} \right) = -\frac{\Delta H}{RT} + \frac{\Delta S}{R} \quad (23)$$

## 3. Results and discussion

### 3.1. Adsorbent characterization

The FTIR of the SMDL in the wavelength region of 500–4,000  $\text{cm}^{-1}$ , before and after dye adsorption is shown in Fig. 2 that confirms the dye adsorption onto the biosorbent surface. An intense peak observed at 3,342  $\text{cm}^{-1}$  corresponds to vibrations at O–H stretch in the hydroxyl

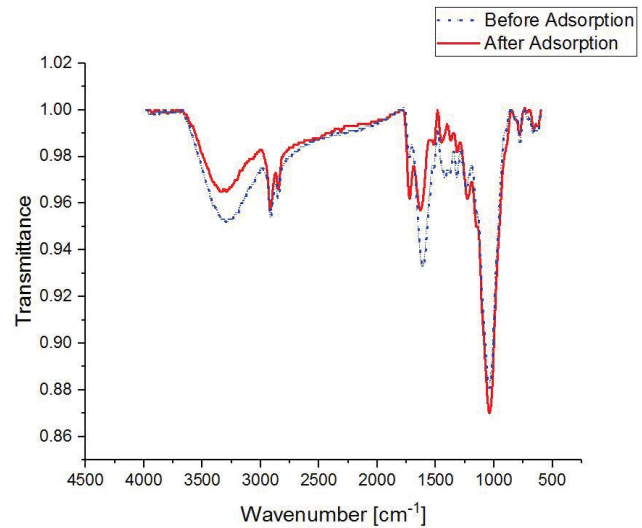
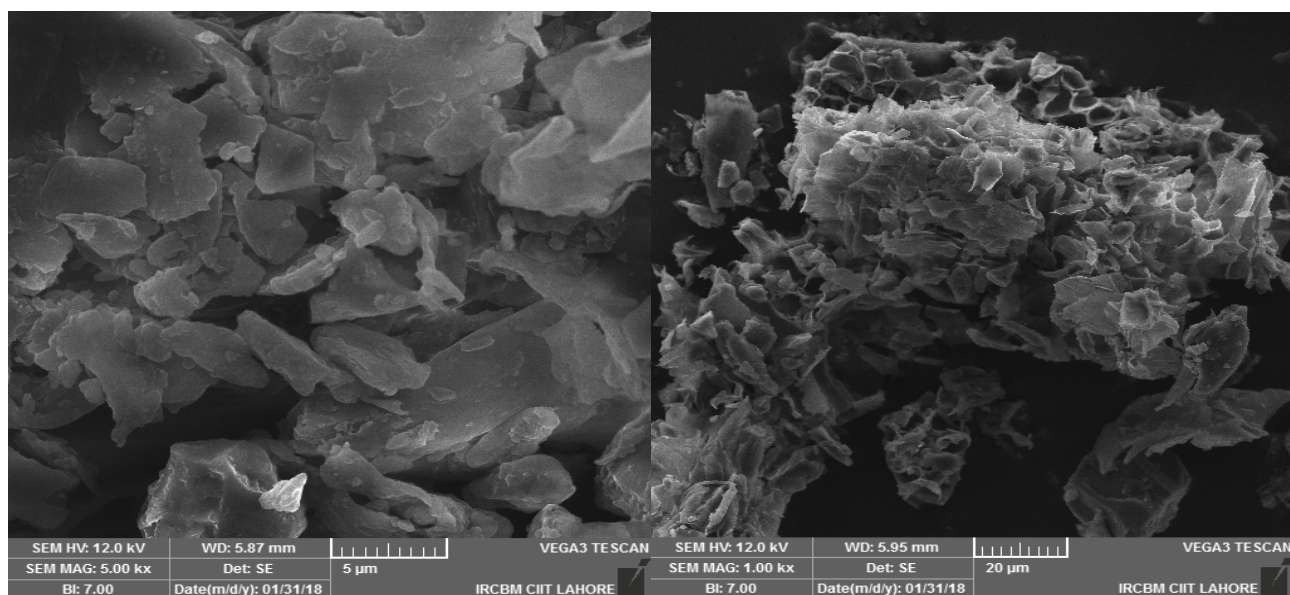


Fig. 2. FTIR spectrum of SMDL.

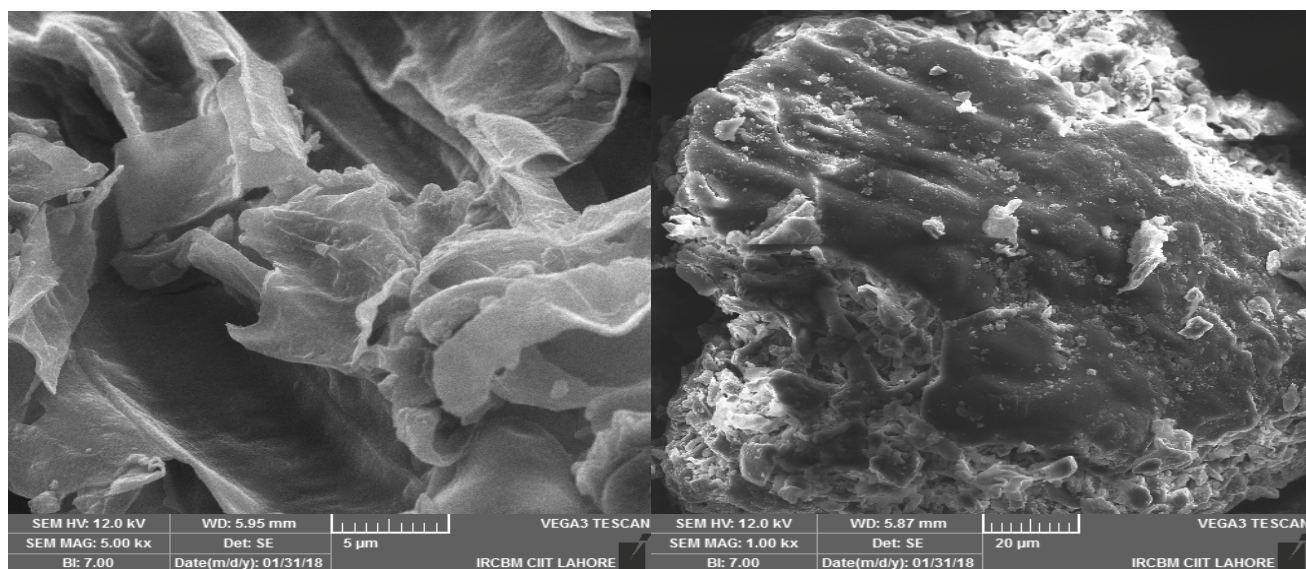
groups present at the biosorbent surface [30]. The peaks obtained at 2,916 and 2,849  $\text{cm}^{-1}$  correspond to the vibration of the C–H stretch in alkanes such as methyl and methylene groups [30,31]. The peaks observed at 1,725 and 1,631  $\text{cm}^{-1}$  are characteristics of carbonyl group C=O [2,30], while peaks in the region 1,450–1,517  $\text{cm}^{-1}$  correspond to aromatic and aliphatic groups and alcohols [21]. A very sharp peak observed at 1,042  $\text{cm}^{-1}$  corresponds to the vibration of carboxylic acids [2,21]. The FTIR spectrum after dye adsorption showed a displacement of peaks in the ranges 1,042–1,050, 1,609–1,725, and 3,242–3,350  $\text{cm}^{-1}$  that gives evidence for the attachment of dye molecules to the functional groups such as carboxylic acid groups, C–H aliphatic groups, and hydroxyl groups [2,30,31].

The morphological texture and surface characteristics of the SMDL are shown by SEM images (Figs. 3(a) and (b)) before and after the dye adsorption. A considerable change in the surface texture of the adsorbent was exhibited by SEM images after dye adsorption. A rough irregular surface morphology with pores was observed before the dye adsorption (Fig. 3(a)). A smoother surface structure obtained after the dye adsorption (Fig. 3(b)) confirms the surface coverage by the dye molecules. Similar morphological changes on dye adsorption have been reported [17]. The elemental composition of SMDL was determined by EDX technique. Figs. 4(a) and (b) and Table 1 show the EDX spectrum and elemental analysis of SMDL before and after the RR-241 biosorption. The EDX spectrum peaks revealed that SMDL is mainly composed of C, O, K, P, Ca, Na, and S. The increase in the weight percent of C from 50.47% to 56.05%, Na from 0.3% to 0.69%, and S from 0.1% to 0.28% confirmed the dye adsorption onto SMDL. So, it is concluded that after RR-241 loading on SMDL the elemental composition altered.

The BET surface area analysis of SMDL exhibited a specific surface area of 4.77  $\text{m}^2/\text{g}$ , an average pore diameter of 29.96  $\text{\AA}$ , a total pore volume of  $6.95 \times 10^{-3} \text{ cm}^3/\text{g}$ . The results showed that SMDL adsorbent can be classified as the mesoporous material as described by International Union of Pure and Applied Chemistry (IUPAC) with pores between 20



(a)



(b)

Fig. 3. SEM images of SMDL (a) without dye adsorption and (b) with dye adsorption.

and  $500\text{\AA}$  [16]. The point of zero charge of SMDL where the net surface charge is zero, determined by pH drift method was to be 5.8.

### 3.2. Effect of pH

The solution pH is the prime factor in the sorption process that controls the dye–biosorbent interaction by altering the surface charge and the functional groups at the surface of biosorbent [32]. The pH influence on dye removal was studied by altering the pH in the range 2–10 (Fig. 5) and it

was revealed that the biosorption process was highly governed by solution pH. The highest dye removal of 94.48% was achieved at  $\text{pH} = 2$ . The dye removal efficiency declined with a rise in pH and negligible dye removal was obtained in alkaline pH. It can be explained by analyzing the RR-241 molecular structure as it contains highly acidic sulfonate ( $-\text{SO}_3$ ) groups that impart anionic character to the dye in solution thus under the strongly acidic conditions, the functional groups on the biosorbent surface are protonated thereby electrostatic interaction of anionic dye may be enhanced [33], while at alkaline pH, therefore, the surface of

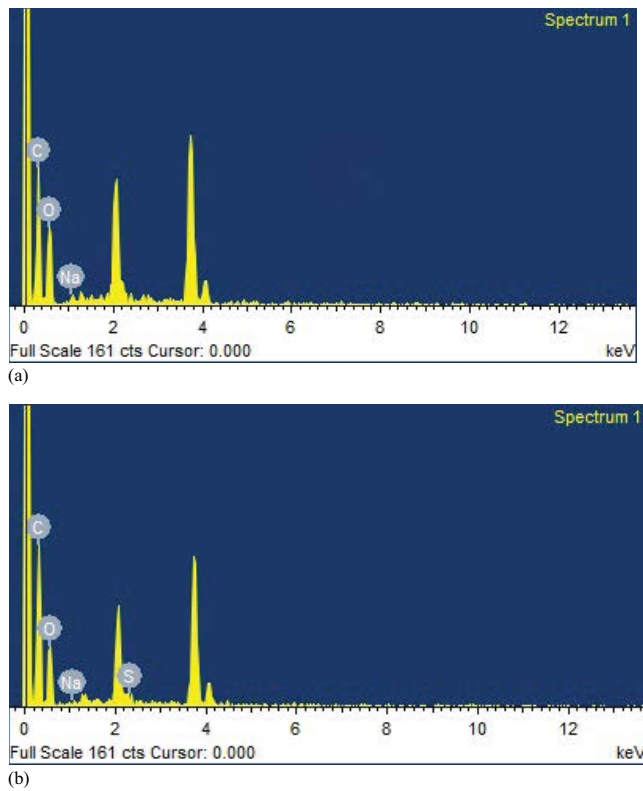


Fig. 4. EDX Spectra of SMDL (a) without dye adsorption and (b) with dye adsorption.

the biosorbent may be deprotonated and negatively charged thereby the electrostatic repulsion of anionic dye reduces biosorption [16].

Moreover, the point of zero charge (when  $pH = pH_{pzc}$ ) of the biosorbent was determined to be 5.8. At  $pH < pH_{pzc}$  the surface of biosorbents gets positively charged and electrostatic interactions of dye molecules increases by  $\pi$ - $\pi$  stacking, dipole-dipole interactions, and hydrogen bonding [16]. The obtained results were found consistent with those reported by Refs. [1,3,31].

### 3.3. Effect of SMDL dosage

The optimum SMDL dosage was determined by varying the doses at 4, 8, 12, 16, and 20 g/L. The obtained results (Fig. 5) revealed that with a rise in biosorbent dose from 4 to

Table 1  
EDX elemental composition of SMDL

Element	Weight %	
	Before RR-241 adsorption	After RR-241 adsorption
C	50.47	56.05
O	48.73	43.37
Na	0.3	0.69
S	0.1	0.28

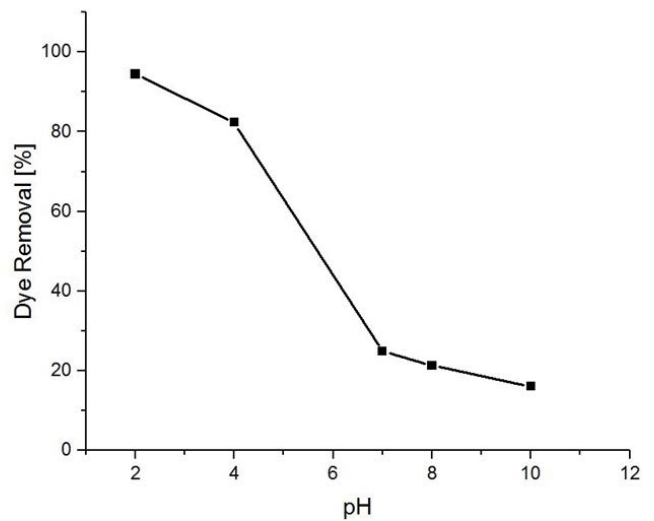


Fig. 5. Effect of pH on the decolorization of RR-241 ( $C_o(RR-241) = 50 \text{ mg/L}$ ;  $T = 30^\circ\text{C}$ ; SMDL dosage = 8 g/L; Vol. = 50 mL; agitation = 200 rpm; time = 120 min).

8 g/L, the RR-241 removal significantly increased from 69.27% to 94.48%. The 8 g/L dose was selected as optimum because the further increase in dose was found to have no significant effect in dye removal at studied initial concentration and dye removal was stabilized (Fig. 6). The results further reveal that the initial sharp rise in the RR-241 removal with biosorbents dose can be ascribed to the high concentration gradients and increase in the availability of sorption sites with biosorbents dosage till the optimum dosage was achieved, when all the sorption sites become saturated and further increase in the biosorbents dosage causes the aggregation of adsorbent particles which leads to a slight reduction in dye removal efficiency [2,34]. Similar behavior for the dye biosorption onto lignocellulosic materials was reported [31,35].

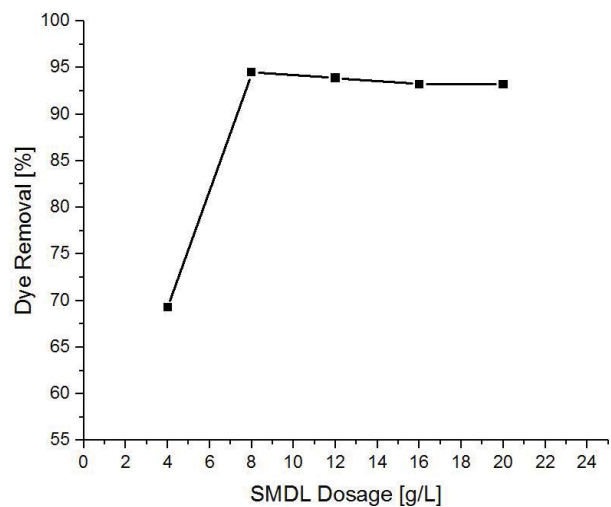


Fig. 6. Effect of SMDL dosage on the decolorization of RR-241 ( $C_o(RR-241) = 50 \text{ mg/L}$ ;  $T = 30^\circ\text{C}$ ; pH = 2; Vol. = 50 mL; agitation = 200 rpm; time = 120 min).

### 3.4. Effect of initial dye concentration and contact time

The results presented in Fig. 7 show that dye removal decreased with a rise in RR-241 initial concentration. It may be explained as the specific dosage of biosorbent provides a fixed number of sorption sites for the dye molecules and at the low dye concentration the removal efficiency was high due to availability of vacant sorption sites and with an increase in dye concentration the sorption sites are covered with dye molecules and become saturated as further increase in dye concentration causes a decrease in removal efficiency [36].

The contact time for the biosorption showed a significant increase in the dye removal efficiency with elongated contact time (Fig. 7). The biosorption kinetics for dye removal was very fast till 60 min and then a sluggish removal was observed until the equilibrium achieved. It may be explained as initially the driving force for the mass transfer between the aqueous phase and biosorbents was high to overcome the diffusion resistance and as the biosorption proceeds the driving force decreases that slows down the dye removal kinetics [19]. So, the initial RR-241 concentration of 50 mg/L and a contact time of 100 min were selected as the optimum concentration and equilibrium time. The experimental results were found in agreement as reported by Refs. [33,35].

### 3.5. Effect of temperature

The dye biosorption was studied at various temperatures of 293, 303, 313, and 323 K with the initial dye concentration of 10, 30, 50, and 70 mg/L, respectively. The obtained results (Fig. 8) showed that the elevation in temperature increased the dye removal, revealing the endothermic nature of process with a maximum removal of 97.05% at 323 K with 10 mg/L initial concentration. The increase in dye removal with temperature can be explained on the following basis. The rise in temperature may cause a decrease in the viscosity of the aqueous solution thereby increasing the mass transfer rate [30]. The dye sorption capacity is increased first due to rise

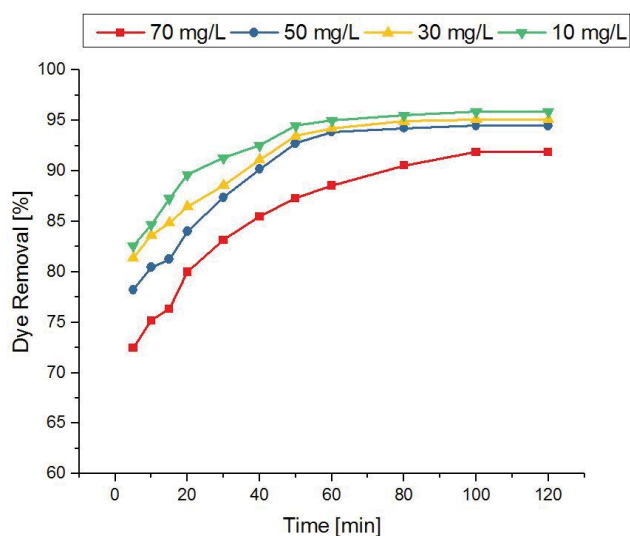


Fig. 7. Effect of initial concentration of RR-241 with contact time (SMDL dosage = 8 g/L;  $T = 30^{\circ}\text{C}$ ;  $\text{pH} = 2$ ; Vol. = 50 mL; agitation = 200 rpm; time = 120 min).

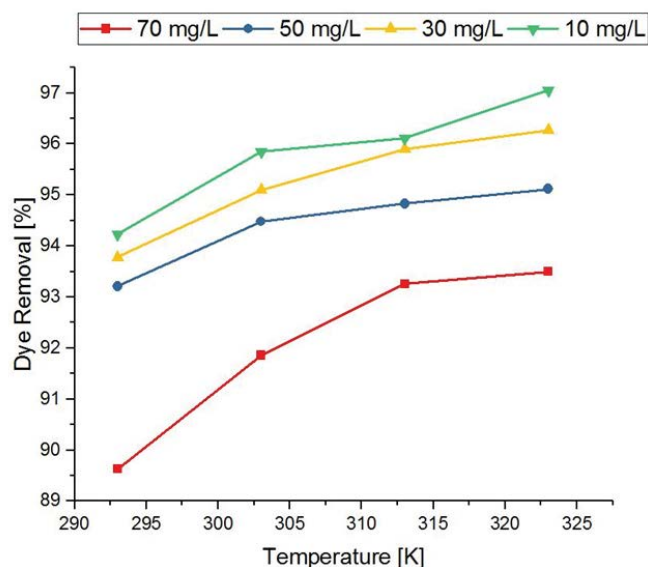


Fig. 8. Effect of temperature on decolorization of RR-241v ( $C_{o(\text{RR-241})} = 50 \text{ mg/L}$ , SMDL dosage = 8 g/L;  $\text{pH} = 2$ ; Vol. = 50 mL; agitation = 200 rpm; time = 120 min).

in molecular kinetic energy that enhances the adsorbent-adsorbate collision frequency increasing sorption and also bond breakage at the surface functional groups occur at elevated temperatures that makes more sorption sites available for dye sorption [19].

### 3.6. Adsorption kinetics

The kinetic plots for the experimental data of biosorption of RR-241 on SMDL for Elovich equation, pseudo-first-order kinetic model, pseudo-second-order kinetic model, and intraparticle diffusion models are given in Fig. 9. The calculated values of the kinetic model's parameters are given in Table 2. The pseudo-second-order model gave the best fit for the biosorption kinetics with highest values of  $R^2$  of 0.999. The obtained values of the rate constant  $K_2$  were high for the pseudo-second-order model as compared with other models, with the largest value of  $K_2$  of 0.606 g/mg min (Table 2). Moreover, a close fit was obtained between the calculated values of adsorption capacity  $q_{e,\text{cal}}$  and experimental values of adsorption capacity  $q_{e,\text{exp}}$  indicating the suitability of pseudo-second-order kinetics. The order of fitness of pseudo-second-order kinetic model > intraparticle diffusion model > pseudo-first-order kinetic model > Elovich model was obtained for kinetic studies of biosorption of RR-241 on SMDL. The pseudo-second-order kinetics of biosorption of RR-241 on SMDL suggests that the rate controlling step may be the chemisorption [6]. A high influence of operating pH on the dye removal (Fig. 5) reveals that the ion exchange mechanism [34] is dominant in the biosorption of RR-241 on SMDL and a high positive value of the  $\Delta H^\circ$  indicates the irreversible adsorption process [34].

### 3.7. Adsorption isotherms

The isotherm model plots for the equilibrium data of biosorption of RR-241 on SMDL are presented in Fig. 10.

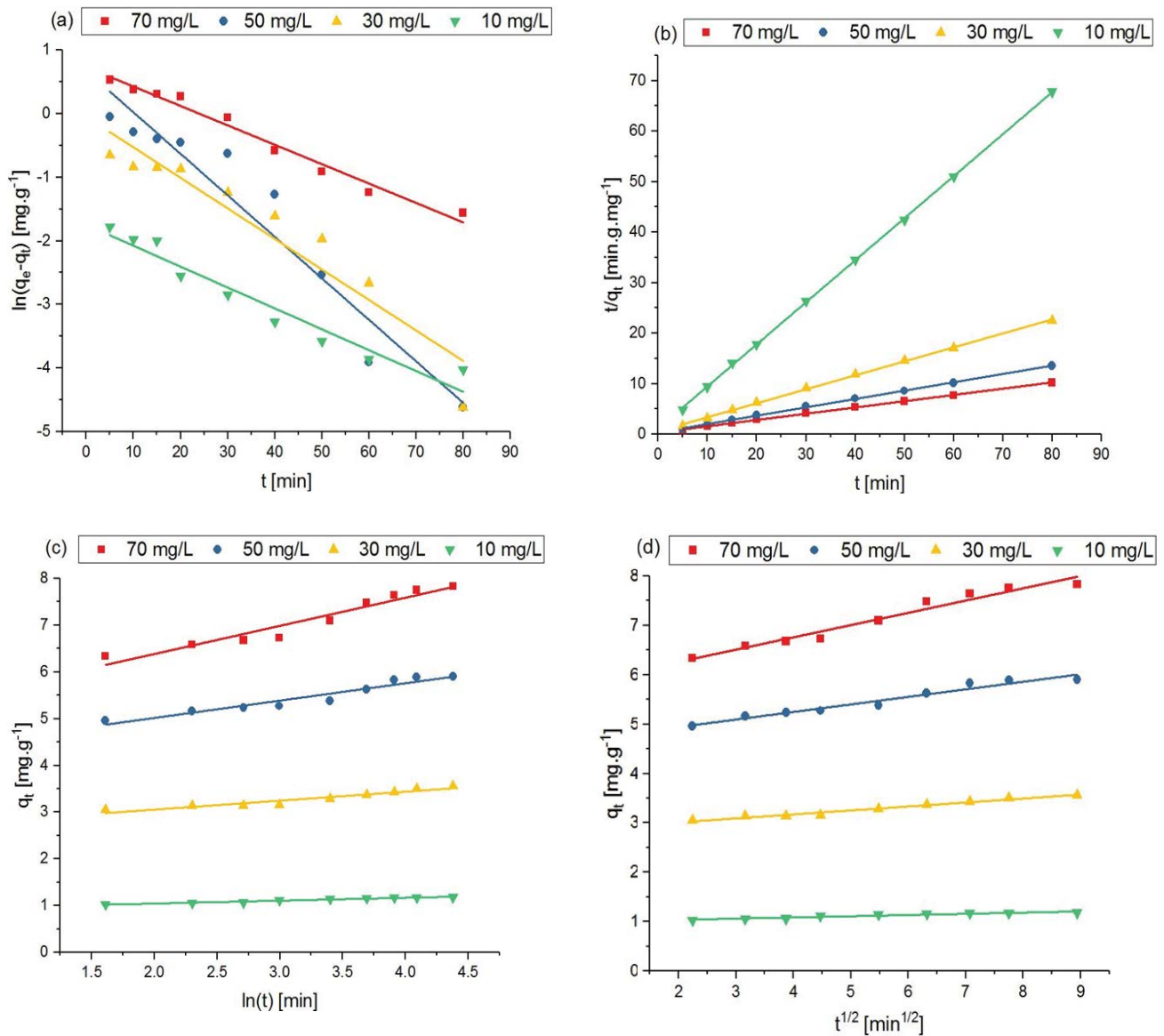


Fig. 9. Kinetic models plots for the biosorption of RR-241: (a) pseudo-first-order model, (b) pseudo-second-order model, (c) Elovich model, and (d) intraparticle diffusion model.

Table 2  
Kinetic parameters for the biosorption of RR-241 on SMDL

Initial dye concentration (mg/L)	Kinetic models									
	Pseudo-first-order model		Pseudo-second-order model		Elovich model			Intraparticle diffusion model		
	$K_1$ (min <sup>-1</sup> )	$R^2$	$K_2$ (g/mg/min)	$H$ (mg/g/min)	$R^2$	$\alpha$ ( $\times 10^3$ ) (mg/g/min)	$\beta$ (g/mg)	$R^2$	$K_{dif}$ (mg/g/min <sup>1/2</sup> )	$R^2$
70	0.0305	0.978	0.0438	2.845	0.999	3.3	1.661	0.936	0.2484	0.965
50	0.0652	0.93	0.0732	2.679	0.999	37.7	2.697	0.929	0.1529	0.957
30	0.048	0.902	0.1282	1.671	0.999	223.79	5.227	0.911	0.0804	0.975
10	0.0328	0.941	0.6059	0.874	0.999	204.64	16.26	0.952	0.0244	0.905

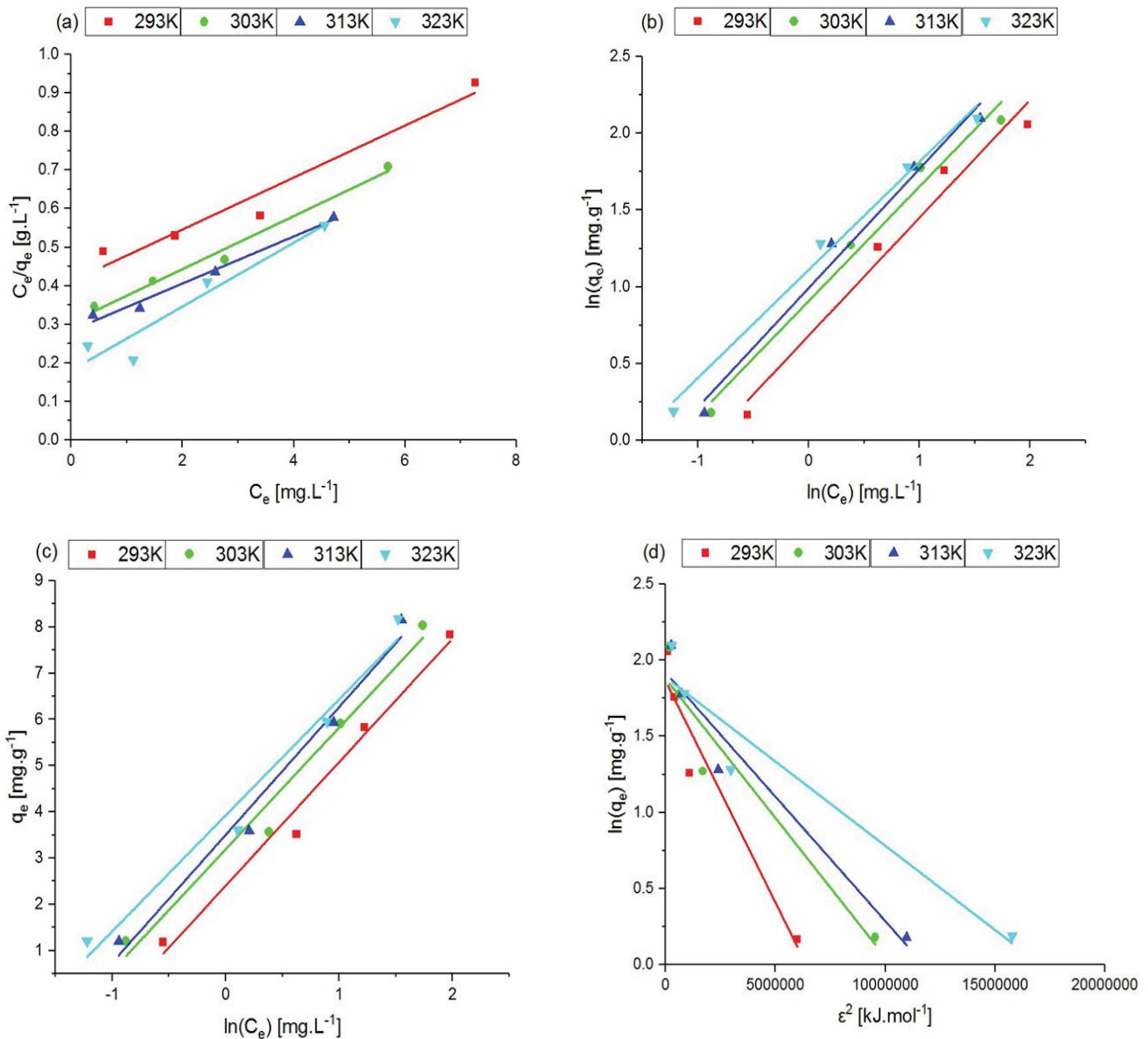


Fig. 10. Isotherm models plots for the biosorption of RR-241: (a) Langmuir model, (b) Freundlich model, (c) Temkin model, and (d) Dubinin–Radushkevich model.

The isotherm model’s parameters values are given in Table 3. The Freundlich isotherm model gave the best fit for the biosorption of RR-241 on SMDL with the highest value of  $R^2$  of 0.99 indicating the heterogeneous nature of adsorption. A high value of Freundlich constant  $K_f$  of 3.04 indicated that high adsorbent loading can be achieved. Moreover, the value of Freundlich intensity parameter  $1/n$  was found to be 0.704 which is less than 1 implies that monolayer adsorption is favorable.

The maximum monolayer adsorption capacity  $q_m$  of SMDL for RR-241 as calculated from Langmuir isotherm was 16.39 mg/g. Moreover, the value of  $R_L$  separation factor was found within 0 and 1, showing that adsorption is favorable. The order of fitness of Freundlich isotherm model > Temkin isotherm model > Langmuir isotherm model > D-R isotherm

model was obtained for equilibrium isotherm studies of biosorption of RR-241 on SMDL.

### 3.8. Adsorption thermodynamics

The plot of the Van’t Hoff equation for the biosorption of RR-241 on SMDL is shown in Fig. 11, while the calculated values of thermodynamic parameters of free energy change ( $\Delta G^\circ$ ), enthalpy change ( $\Delta H^\circ$ ), and entropy change ( $\Delta S^\circ$ ) are shown in Table 4. At all the studied temperatures (293, 303, 313, and 323 K), the free energy change ( $\Delta G^\circ$ ) negative values indicate that the biosorption of RR-241 on SMDL is a spontaneous reaction and feasible. The determined value of enthalpy change ( $\Delta H^\circ$ ) was positive (14.39 kJ/mol) that shows that biosorption of RR-241 on SMDL is an endothermic process.

Table 3  
Isotherm parameters for the biosorption of RR-241 on SMDL

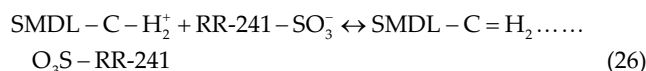
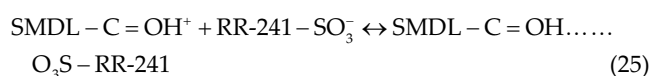
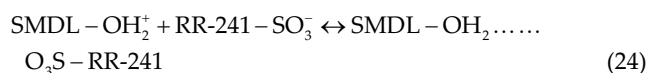
Temperature (K)	Isotherm models											
	Langmuir model			Freundlich model			Temkin model			Dubinin–Radushkevich model		
	$K_L$ (L/mg)	$q_m$ (mg/g)	$R^2$	$K_F$ (mg/g)(L/mg) <sup>1/n</sup>	1/n	$R^2$	$K_T$ (L/mg)	$b$	$R^2$	$\beta$ (mol <sup>2</sup> /kJ <sup>2</sup> )	$q_m$ (mg/g)	$R^2$
293	0.164	14.84	0.953	1.98	0.768	0.972	2.46	0.911	0.984	$3 \times 10^{-7}$	6.44	0.935
303	0.225	14.56	0.985	2.48	0.745	0.982	3.37	0.958	0.978	$2 \times 10^{-7}$	6.54	0.931
313	0.215	16.39	0.985	2.7	0.776	0.984	3.55	0.941	0.981	$2 \times 10^{-7}$	6.82	0.947
323	0.458	12.08	0.916	3.04	0.704	0.990	4.78	1.07	0.974	$1 \times 10^{-7}$	6.61	0.934

A positive value (0.055 kJ/mol K) of entropy change ( $\Delta S^\circ$ ) shows that the rise in randomness occurred at the solid–liquid molecular interface due to the biosorption of RR-241 on SMDL.

### 3.9. Mechanism of RR-241 adsorption on SMDL

The adsorption of the dye depends on various factors such as pH, the surface area of the adsorbent, surface charges on the adsorbate, and the adsorbent and nature of the adsorbent [31,37,38]. The RR-241 contains the sulfonic groups in its structure (Fig. 1) that impart anionic character to the dye thereby produces anions ( $\text{SO}_3^-$ ) in the aqueous solution [19,37]. The SMDL is a lignocellulosic-based material containing various negatively charged functional groups on its surface as revealed by FTIR such as the hydroxyl, carbonyl, and carboxyl groups (Fig. 2). The possible mechanism of RR-241 adsorption on the SMDL may be the ionic interactions among the RR-241 ions ( $\text{RR241-SO}_3^-$ ) and the SMDL surface functional groups such as hydroxyl (SMDL-OH), carbonyl (SMDL-C=O), and aliphatic (SMDL-C-H) groups [19,37]. In this investigation, the maximum adsorption of RR-241 on SMDL was observed at acidic pH (Fig. 5). The

point of zero charge of SMDL showed that at  $\text{pH} < \text{pH}_{\text{pzc}}$  the surface of SMDL becomes protonated due to the presence of  $\text{H}^+$  ions that enhances the negatively charged RR-241 adsorption due to opposite charges [31]. The possible ionic interactions at strongly acidic pH among the dye ions and the SMDL surface protonated groups (hydroxyl, carbonyl, and aliphatic) are shown as follows [19,37]:



Under alkaline pH, the  $\text{OH}^-$  ions increases in the aqueous solution that cause a reduction in the dye adsorption by competing with the RR-241 anions at the sorption sites [19,37]. At  $\text{pH} > \text{pH}_{\text{pzc}}$  the electrostatic repulsion [19,37] between the RR-241 anions and the negatively charged SMDL surface reduces the dye adsorption as revealed in Fig. 5. Thus, it has been suggested that the electrostatic interactions play a vital role in the mechanism of RR-241 adsorption on SMDL. [31,37,38]

### 3.10. Comparison with literature data

The comparison of the adsorption capacities from various studies reported on the use of leaves as low-cost

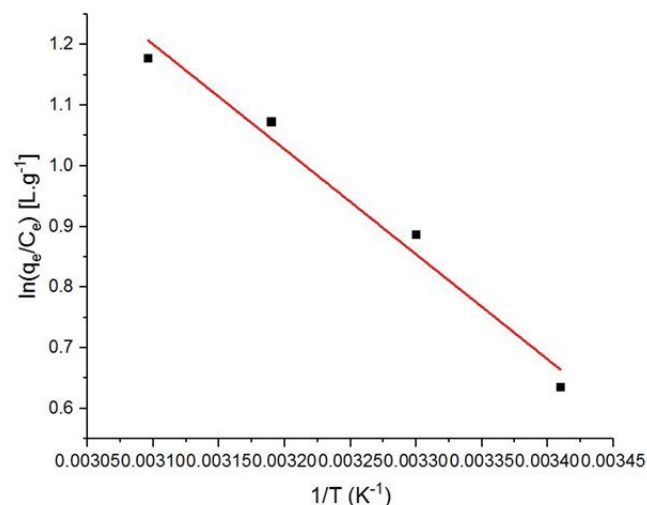


Fig. 11. Plot of  $\ln(q_e/C_e)$  versus  $1/T$  for the estimation of thermodynamic parameters for the biosorption of RR-241 on SMDL.

Table 4  
Thermodynamic parameters for the biosorption of RR-241 on SMDL

Temperature (K)	$\Delta G^\circ$ (kJ/mol)	$\Delta H^\circ$ (kJ/mol)	$\Delta S^\circ$ (kJ/mol/K)
293	-1.55		
303	-2.23		
313	-2.79	14.39	0.055
323	-3.16		

Table 5  
Comparison of adsorption capacities of various leaves as low cost biosorbents for dye removal

Leaves biosorbent	Type of dye	Adsorption capacity (mg/g)	Reference
Neem leaf	Methylene Blue (cationic)	8.76	[39]
<i>Posidonia oceanica</i> (L.) Leaf	Reactive Cibacron Red FNR (anionic)	4.252	[43]
Guava leaves	Auramine (cationic)	8	[41]
<i>Paulownia tomentosa</i> Steud. Leaf	Acid Orange 52 (anionic)	10.5	[40]
Mango ( <i>Mangifera indica</i> ) leaf	Rhodamine B (cationic)	3.31	[44]
Jackfruit leaf	Amido Black 10B (anionic)	3.7	[42]
Indian spinach leaf powder	Malachite Green (cationic)	2.54	[45]
<i>Sapindus mukorossi</i> dead leaves	Reactive Red 241 (anionic)	8.18	Present work

biosorbents for the dye removal is presented in Table 5. It is evident that the dye adsorption capacity of 8.18 mg/g of SMDL is comparable with those reported by many researchers [39–45]. The results indicate the biosorption potential of SMDL for application as efficient, environment-friendly, and cheaper biosorbent for the treatment of RR-241 in wastewater.

The high adsorption efficiencies of anionic dyes on the natural biosorbent materials at strongly acidic pH have been previously reported. The highest dye removal at pH 2 was reported for Amido black dye ( $\approx 86\%$ ) on natural Jackfruit leaf [42], reactive red 194 ( $\approx 68\%$ ) on cupuassu shell [31], reactive red 141 (85%) on pecan nutshell biochar [12], and congo red (37.88 mg/g) on modified *Glossogyne tenuifolia* leaves [17]. The increase in the sorption sites upto optimum adsorbent dosage enhanced the dye removal as reported by researchers [17,18,39]. The decrease in dye % removal with the increase in initial dye concentration has been reported [41,42]. The enhancement of dye removal with the decrease in viscosity at higher temperature has been reported [21,41]. The results presented in this investigation also indicate similar trends for the removal of RR-241 on SMDL. Therefore, the results were found in true agreement with those previously reported in research.

#### 4. Conclusions

The work identified the SMDL as natural, cheaper, and effective biosorbent for the treatment of RR-241 in aqueous solution. The FTIR characterization of SMDL showed that the  $-\text{COOH}$ ,  $-\text{C}=\text{O}$ , and  $-\text{OH}$  functional groups were mainly present at the surface that took part in the interaction with RR-241 as sorption sites. The SEM images indicate the irregular porous surface morphology of SMDL. The dye sorption was influenced by various parameters such as pH, SMDL dosage, initial RR-241 concentration, temperature, and contact time. The results further indicate that the dye sorption was favored at acidic pH with a maximum at pH 2. The rise in temperature favored the dye sorption that revealed the endothermic nature of biosorption. Kinetic study revealed that adsorption kinetics follows the pseudo-second-order model with the highest rate constant of 0.606 g/mg/min. The equilibrium data gave the best fit with the Freundlich isotherm model. The thermodynamic parameters indicate that the biosorption of RR-241 on SMDL was a spontaneous and feasible

process ( $\Delta G^\circ$  values being negative), endothermic in nature ( $\Delta H^\circ = 14.39$  kJ/mol), and showed increased randomness at the solid–liquid interface ( $\Delta S^\circ = 0.055$  kJ/mol K).

#### Acknowledgment

The authors gratefully acknowledge the technical support and financial assistance provided by the University of Engineering and Technology Lahore Pakistan for this research work through project no. ORIC/100-ASRB/1977.

#### Symbols

$C_o$	—	Initial dye concentration, mg/L
$C_t$	—	Dye concentration at time $t$ , mg/L
$C_e$	—	Equilibrium dye concentration, mg/L
$V$	—	Volume of aqueous dye solution, L
$M$	—	Mass of adsorbent, g
$q_t$	—	Adsorption capacity at time $t$ , mg/g
$q_e$	—	Adsorption capacity at equilibrium, mg/g
$q_m$	—	Maximum adsorption capacity, mg/g
$K_1$	—	First-order rate constant, $\text{min}^{-1}$
$K_2$	—	Second-order rate constant, g/mg/min
$h$	—	Initial biosorption rate for second-order kinetics, mg/g/min
$\alpha$	—	Initial rate of adsorption, mg/g/min
$\beta$	—	Desorption constant, g/mg
$K_{\text{dif}}$	—	Intraparticle diffusion model rate constant, mg/g/min <sup>1/2</sup>
$C$	—	Extent of film diffusion, mg/g
$K_L$	—	Langmuir constant, L/mg
$R_L$	—	Separation factor
$K_f$	—	Freundlich constant
$1/n$	—	Freundlich intensity parameter
$R$	—	Gas constant, 8.314 J/mol/K
$T$	—	Absolute temperature, K
$K_T$	—	Temkin binding constant, L/g
$b$	—	Constant related to heat of adsorption
$\Delta G$	—	Free energy change, kJ/mol
$\Delta H$	—	Enthalpy change, kJ/mol
$\Delta S$	—	Entropy change, kJ/mol/K

#### References

- [1] S.P.D.M. Blanco, F.B. Scheufele, A.N. Módenes, F.R. Espinoza-Quíñones, P. Marin, A.D. Kroumov, C.E. Borba, Kinetic

- equilibrium and thermodynamic phenomenological modeling of reactive dye adsorption onto polymeric adsorbent, *Chem. Eng. J.*, 307 (2017) 466–475.
- [2] J. Liu, Z. Wang, H. Li, C. Hu, P. Raymer, Q. Huang, Effect of solid state fermentation of peanut shell on its dye adsorption performance, *Bioresour. Technol.*, 249 (2017) 307–314.
  - [3] Y.O. Khaniabadi, H. Basiri, H. Nourmoradi, M.J. Mohammadi, A.R. Yari, S. Sadeghi, A. Amrane, Adsorption of Congo Red Dye from aqueous solutions by montmorillonite as a low-cost adsorbent, *Int. J. Chem. React. Eng.*, 16 (2017) 16–21.
  - [4] S. Ziane, F. Bessaha, K. Marouf-Khelifa, A. Khelifa, Single and binary adsorption of reactive black 5 and Congo red on modified dolomite: performance and mechanism, *J. Mol. Liq.*, 249 (2018) 1245–1253.
  - [5] B. Zhao, W. Xiao, Y. Shang, H. Zhu, R. Han, Adsorption of light green anionic dye using cationic surfactant-modified peanut husk in batch mode, *Arab. J. Chem.*, 10 (2017) S3595–S3602.
  - [6] M.A.M. Salleh, D.K. Mahmoud, W.A.W.A. Karim, A. Idris, Cationic and anionic dye adsorption by agricultural solid wastes: a comprehensive review, *Desalination*, 280 (2011) 1–13.
  - [7] J. Shi, B. Zhang, S. Liang, J. Li, Z. Wang, Simultaneous decolorization and desalination of dye wastewater through electrochemical process, *Environ. Sci. Pollut. Res. Int.* 25 (2018) 8455–8464.
  - [8] M. Gagol, A. Przyjazny, G. Boczkaj, Wastewater treatment by means of advanced oxidation processes based on cavitation – a review, *Chem. Eng. J.* 338 (2018) 599–627.
  - [9] T.K.F.S. Freitas, C.A. Almeida, D.D. Manholer, H.C.L. Geraldino, M.T.F. de Souza, J.C. Garcia, Review of utilization plant-based coagulants as alternatives to textile wastewater treatment, *Text. Sci. Clothing Technol.* 1 (2018) 27–79.
  - [10] M. Sarvajith, G.K.K. Reddy, Y.V. Nancharaiah, Textile dye biodecolourization and ammonium removal over nitrite in aerobic granular sludge sequencing batch reactors, *J. Hazard. Mater.*, 342 (2018) 536–543.
  - [11] J. He, A. Cui, S. Deng, J.P. Chen, Treatment of methylene blue containing wastewater by a cost-effective micro-scale biochar/polysulfone mixed matrix hollow fiber membrane: performance and mechanism studies, *J. Colloid Interface Sci.*, 512 (2018) 190–197.
  - [12] M.A. Zazycki, M. Godinho, D. Perondi, E.L. Foletto, G.C. Collazzo, G.L. Dotto, New biochar from pecan nutshells as an alternative adsorbent for removing reactive red 141 from aqueous solutions, *J. Cleaner Prod.*, 171 (2018) 57–65.
  - [13] A. Regti, M.R. Laamari, S.-E. Stiriba, M. El Haddad, Use of response factorial design for process optimization of basic dye adsorption onto activated carbon derived from *Persea* species, *Microchem. J.*, 130 (2017) 129–136.
  - [14] A. Regti, H.B. El Ayouchi, M.R. Laamari, S.E. Stiriba, H. Anane, M. El Haddad, Experimental and theoretical study using DFT method for the competitive adsorption of two cationic dyes from wastewaters, *Appl. Surf. Sci.*, 390 (2016) 311–319.
  - [15] A. Regti, A. El Kassimi, M.R. Laamari, M. El Haddad, Competitive adsorption and optimization of binary mixture of textile dyes: a factorial design analysis, *J. Assoc. Arab Univ. Basic Appl.*, 24 (2018) 1–9.
  - [16] R.A. Fideles, G.M.D. Ferreira, F.S. Teodoro, O.F.H. Adarme, L.H.M. da Silva, L.F. Gil, L.V.A. Gurgel, Trimellitinated sugarcane bagasse: a versatile adsorbent for removal of cationic dyes from aqueous solution. Part I: Batch adsorption in a monocomponent system, *J. Colloid Interface Sci.*, 515 (2018) 172–188.
  - [17] J.-X. Yang, G.-B. Hong, Adsorption behavior of modified *Glossogyne tenuifolia* leaves as a potential biosorbent for the removal of dyes, *J. Mol. Liq.* 252 (2017) 289–295.
  - [18] M. Kaya, Evaluation of a novel woody waste obtained from tea tree sawdust as an adsorbent for dye removal, *Wood Sci. Technol.*, 52 (2017) 245–260.
  - [19] P.G. Radhakrishnan, S.P. Varghese, B.C. Das, Application of ethylenediamine hydroxypropyl tamarind fruit shell as adsorbent to remove Eriochrome black T from aqueous solutions – kinetic and equilibrium studies, *Sep. Sci. Technol.*, 53 (2017) 417–438.
  - [20] A.E. Ghaly, R. Ananthashankar, M. Alhattab, V.V. Ramakrishnan, Production, characterization and treatment of textile effluents: a critical review, *J. Chem. Eng. Proc. Technol.*, 5 (2013) 1–18.
  - [21] E.A. Khan, Shahjahan, T.A. Khan, Adsorption of methyl red on activated carbon derived from custard apple (*Annona squamosa*) fruit shell: equilibrium isotherm and kinetic studies, *J. Mol. Liq.*, 249 (2018) 1195–1211.
  - [22] S. Lagergren, About the theory of so-called adsorption of soluble substances, *K. Sven. vetensk. akad. handl.*, 24 (1989) 1–39.
  - [23] Y.S. Ho, G. McKay, Sorption of dye from aqueous solution by peat, *Chem. Eng. J.*, 70 (1998) 115–124.
  - [24] Y.B.Z.S.Z. Roginsky, Die katalische oxidation von kohlenmonoxyd auf mangandioxyd, *Acta Phys. Chim.*, 1 (1934) 554–594.
  - [25] W.J. Weber, J.C. Morris, Kinetics of adsorption on carbon from solution, *J. Sanit. Eng. Div. Proc.*, 89 (1962) 31–59.
  - [26] I. Langmuir, The adsorption of gases on plane surface of glass, mica and platinum, *J. Am. Chem. Soc.*, 40 (1918) 1361–1403.
  - [27] H.M.F. Freundlich, Over the adsorption in solution, *J. Phys. Chem.*, 57 (1906) 385–470.
  - [28] M. Temkin, V. Pyzhev, Kinetics of ammonia synthesis on promoted iron catalysts, *Acta Phys. Chim. Sin.*, 12 (1940) 217–222.
  - [29] M.M. Dubinin, The potential theory of adsorption of gases and vapors for adsorbents with energetically non-uniform surface, *Chem. Rev.*, 60 (1960) 235–266.
  - [30] M. Farnane, H. Tounsadi, A. Machrouhi, A. Elhalil, F.Z. Mahjoubi, M. Sadiq, M. Abdennouri, S. Qourzal, N. Barka, Dye removal from aqueous solution by raw maize corncob and H<sub>3</sub>PO<sub>4</sub> activated maize corncob, *J. Water Reuse Desal.* 8 (2017) 214–224.
  - [31] N.F. Cardoso, E.C. Lima, I.S. Pinto, C.V. Amavisca, B. Royer, R.B. Pinto, W.S. Alencar, S.F.P. Pereira, Application of cupuassu shell as biosorbent for the removal of textile dyes from aqueous solution, *J. Environ. Manage.*, 92 (2011) 1237–1247.
  - [32] F.C. Silva, L.C.B. Lima, R.D.S. Bezerra, J.A. Osajima, E.C.S. Filho, Use of cellulosic materials as dye adsorbents – a prospective study, *Intech Open* 1 (2015) 115–132.
  - [33] H. Singh, G. Chauhan, A.K. Jain, S.K. Sharma, Adsorptive potential of agricultural wastes for removal of dyes from aqueous solutions, *J. Environ. Chem. Eng.*, 5 (2017) 122–135.
  - [34] A. Regti, M.R. Laamari, S.-E. Stiriba, M. El Haddad, Removal of Basic Blue 41 dyes using *Persea americana*-activated carbon prepared by phosphoric acid action, *Int. J. Ind. Chem.*, 8 (2016) 187–195.
  - [35] M.E. Mahmoud, G.M. Nabil, N.M. El-Mallah, H.I. Bassiouny, S. Kumar, T.M. Abdel-Fattah, Kinetics, isotherm, and thermodynamic studies of the adsorption of reactive red 195 A dye from water by modified Switchgrass biochar adsorbent, *J. Ind. Eng. Chem.*, 37 (2016) 156–167.
  - [36] M. El Haddad, R. Mamouni, N. Saffaj, S. Lazar, Evaluation of performance of animal bone meal as a new low cost adsorbent for the removal of a cationic dye Rhodamine B from aqueous solutions, *J. Saudi Chem. Soc.*, 20 (2016) S53–S59.
  - [37] G.A.C. Ribeiro, D.S.A. Silva, C.C. dos Santos, A.P. Vieira, C.W.B. Bezerra, A.A. Tanaka, S.A.A. Santana, Removal of Remazol brilliant violet textile dye by adsorption using rice hulls, *Polímeros*, 27 (2017) 16–26.
  - [38] H.N. Tran, S.-J. You, T.V. Nguyen, H.-P. Chao, Insight into the adsorption mechanism of cationic dye onto biosorbents derived from agricultural wastes, *Chem. Eng. Commun.*, 204 (2017) 1020–1036.
  - [39] K.G. Bhattacharyya, A. Sharma, Kinetics and thermodynamics of Methylene Blue adsorption on Neem (*Azadirachta indica*) leaf powder, *Dyes Pigm.*, 65 (2005) 51–59.
  - [40] F. Deniz, S.D. Saygideger, Equilibrium, kinetic and thermodynamic studies of acid Orange 52 dye biosorption by *Paulownia tomentosa* Steud. leaf powder as a low-cost natural biosorbent, *Bioresour. Technol.*, 101 (2010) 5137–5143.
  - [41] R.W. Gaikwad, S.A.M. Kinldy, Studies on auramine dye adsorption on psidium guava leaves, *Korean J. Chem. Eng.*, 26 (2009) 102–107.

- [42] A.K. Ojha, V.K. Bulasara, Adsorption characteristics of jackfruit leaf powder for the removal of Amido black 10B dye, *Environ. Prog. Sustainable Energy*, 34 (2015) 461–470.
- [43] M.C. Ncibi, B. Mahjoub, M. Seffen, Studies on the biosorption of textile dyes from aqueous solutions using *Posidonia oceanica* (L.) leaf sheath fibres, *Adsorpt. Sci. Technol.*, 24 (2006) 461–473.
- [44] T.A. Khan, S. Sharma, I. Ali, Adsorption of Rhodamine B dye from aqueous solution onto acid activated mango (*Mangifera indica*) leaf powder: equilibrium, kinetic and thermodynamic studies, *J. Toxicol. Environ. Health Sci.*, 3 (2011) 286–297.
- [45] O.M. Atoyebi, O.S. Bello, Indian spinach leaf powder as adsorbent for Malachite Green dye removal from aqueous solution, *Cov. J. Phys. Life Sci.*, 2 (2014) 54–67.